Frontiers in Bioscience Landmark

Front. Biosci. (Landmark Ed) **2026**; 31(4): 49862
https://doi.org/10.31083/FBL49862

Original Research

Emodin Alleviates Lipid Accumulation and Renal Tubular Injury in Rats With DN via Inhibiting HIF-1α Expression

Ying Wang[1], Xue Deng[1], Qian-wen Zhu[1,2], Jing Zhang[1], Zhi-wei Qian[1], Fang Gao[1], Shu-qin Zhan[1], Chao Wu[1], Lin Wang[1], Shu Li[1], Ze-bo Hu[1,*]

[1]Department of Pathophysiology, School of Basic Medical Sciences, Wannan Medical University, 241002 Wuhu, Anhui, China
[2]Department of Clinical Laboratory, Meixian People's Hospital, 722300 Baoji, Shaanxi , China
*Correspondence: huzb0007@163.com (Ze-bo Hu)
Academic Editor: Moo-Ho Won
Submitted: 9 January 2026 Revised: 1 March 2026 Accepted: 6 March 2026 Published: 21 April 2026

Abstract

Background: Our previous study verified that lipid nephrotoxicity mediated by hypoxia-inducible factor-1 alpha (HIF-1α) activation aggravates diabetic tubular injury. This study investigated whether emodin, an inhibitor of HIF-1α, improves tubular injury by reducing lipid accumulation in diabetic tubules, and examined its underlying mechanism. **Methods**: Type 1 diabetic rats were administered 40 mg/kg emodin by gavage daily. For the *in vitro* study, HK-2 cells were pretreated with emodin for 6 h and then stimulated with HIF-1α activator cobalt chloride ($CoCl_2$). **Results**: *In vivo*, emodin significantly downregulated HIF-1α protein expression in the kidneys of rats with diabetes. Emodin treatment substantially attenuated tubular pathological damage and reduced 24-h urinary total protein levels and the urinary albumin-to-creatinine ratio in rats with diabetes, accompanied by decreased expression of transforming growth factor-beta 1 (TGF-β1) and connective tissue growth factor (CTGF). Meanwhile, lipid accumulation and mitochondrial dysfunction in diabetic kidneys markedly improved after emodin treatment. Similarly, *in vitro*, emodin effectively reduced HIF-1α protein expression in $CoCl_2$-treated HK-2 cells. Moreover, emodin ameliorated lipid accumulation, cellular injury, and mitochondrial homeostasis imbalance in these cells. **Conclusion**: These data demonstrate that emodin prevents lipid accumulation and cellular injury in diabetic tubular epithelial cells, possibly by inhibiting HIF-1α activation and exerting a protective effect on mitochondria.

Keywords: emodin; diabetic nephropathy; hypoxia-inducible factor-1 alpha; lipid droplets; kidney tubules

1. Introduction

As a chronic microvascular complication arising from diabetes, diabetic nephropathy (DN) ranks among the most severe manifestations of the disease and now stands as the predominant cause of end-stage renal disease on a global scale [1]. In recent years, because the progress of renal insufficiency is closely linked with tubular atrophy and interstitial fibrosis, more and more attention has been paid the impact of tubular lesions on DN [2]. Despite ongoing efforts to develop novel therapies targeting renal interstitial fibrosis in clinical studies, the side effects of these drugs emphasize the necessity to further explore the underlying mechanisms of diabetic tubulopathy.

Toxic lipid intermediates accumulate in nonadipose tissues (kidney, liver, heart, pancreas, and skeletal muscle), leading to lipotoxicity. It commonly causes cellular dysfunction and even death [3]. Kimmelstiel and colleagues first reported the lipid accumulation in the proximal tubules of diabetic kidneys [4], which contributed to DN progression in type 1 and 2 diabetic models [5,6]. The deposition of toxic lipid intermediates in proximal tubules expedited cellular apoptosis, contributing to tubular atrophy in the progression of chronic kidney disease [7]. Various mechanisms referring to increased *de novo* lipogenesis, lipid uptake, synthesis, and decreased fatty acid oxidation caused lipid accumulation in tubules [8].

Our previous study indicated that hypoxia-inducible factor-1 alpha (HIF-1α) activation led to lipid deposition in the tubules of rats with diabetes [9]. Emodin, classified chemically as an anthraquinone derivative, is obtainable from several herbal sources including Rheum palmatum, Polygonum cuspidatum, and cascara buckthorn [10]. Experimental evidence indicates that this compound downregulates HIF-1α expression across multiple tissue types, encompassing cancer cells [11], liver, and skeletal muscle in mice [12]. Moreover, numerous studies have shown that emodin improved lipid metabolism in various animal disease models such as obese mice and mice with acute pancreatitis [13–15]. Thus, whether emodin alleviates lipid accumulation and improves diabetic tubular injury by inhibiting HIF-1α expression needs exploration.

Several previous studies suggested a renoprotective effect of emodin treatment in DN animal models [16]. Emodin prevented podocyte injury in DN by restraining apoptosis and increasing the autophagy of podocytes [17]. Moreover, Ji *et al*. [18] elucidated that emodin protected against DN by inhibiting ferroptosis via restoring nuclear factor E2-related factor 2 expression. Herein, we examined the regulatory role of emodin in lipid metabolism of dia-

betic renal tubular epithelial cells (RTECs) and pursued an in-depth analysis of its operative mechanisms.

2. Materials and Methods

2.1 Animal Studies

Male Sprague–Dawley rats (150 ± 20 g body weight) were obtained from Shanghai Bikai Laboratory Animal Co., Ltd. (Shanghai, China) and maintained under specific-pathogen-free conditions. Following a 7-day acclimatization period, animals were randomly assigned to three experimental groups: normal control (control), diabetic model (DM), and emodin-treated diabetic groups (DM+emodin). To induce type 1 diabetes, 8-week-old rats received a single intraperitoneal dose of streptozotocin (STZ, 60 mg/kg; S0130, Sigma Aldrich, St. Louis, MO, USA) prepared in 0.1 M citrate buffer at pH 4.5, whereas control animals received an equal volume of the vehicle buffer. Successful induction of hyperglycemia was verified 72 h later by fasting blood glucose measurement (>16.7 mmol/L). Emodin-treated rats were orally administered 40 mg/kg emodin (S1312, Selleck, Houston, TX, USA) formulated in 0.5% sodium carboxymethyl cellulose (CMC-Na, S6703, Selleck) once daily by gavage; control and diabetic groups received the corresponding volume of vehicle. The dosage and route of emodin administration have been verified safe and effective [19–21]. Following 8 weeks of treatment, all animals were euthanized for tissue collection. Deep anesthesia was achieved prior to sacrifice through intraperitoneal administration of pentobarbital sodium (2% solution, 45 mg/kg). The animals were then euthanized under deep anesthesia by transcardial perfusion with PBS, which ensured death.

2.2 Cell Culture Studies

The human proximal tubular cell line HK-2, purchased from Wuhan Pricella Biotechnology Co., Ltd., was cultured as described [22]. The cell line was verified by STR profiling and tested negative for mycoplasma. Cells were randomly allocated into three groups: control, cobalt chloride ($CoCl_2$, 100 µmol/L), and $CoCl_2$+ emodin (100 µmol/L $CoCl_2$ and 20 µmol/L emodin) groups. Upon reaching 40–50% cellular confluence, cultures underwent 24 h of serum starvation to achieve cell cycle synchronization, followed by 6 h incubation with either emodin or vehicle (dimethyl sulfoxide, DMSO), and then stimulated with or without $CoCl_2$ (C8661, Sigma–Aldrich) for another 24 h.

2.3 Serum and Urine Measurements

Blood biochemical indicators, including blood glucose levels and lipid profiles, and urinary creatinine levels were determined using automatic analyzers (Rayto, Shenzhen, China). Urinary protein concentrations were quantified via commercial colorimetric assay (E-BC-K252-M, Elabscience, Wuhan, Hubei, China) and then multiplied by 24-h total urine volume to calculate the total protein content in 24-h urine. For albumin detection, a sandwich ELISA protocol was employed according to the manufacturer's specifications. (E-EL-R0025c, Elabscience).

2.4 Transmission Electron Microscopy and Periodic Acid-Schiff (PAS) Staining

Following the procedures outlined in prior studies [23], specimens were processed for PAS staining and ultrastructural evaluation via electron microscopy. In PAS staining, five fields in each rat were randomly selected, and tubulointerstitial damage was quantified using Image-Pro Plus software 6.0 (Media Cybernetics, Rockville, MD, USA).

2.5 Measurement of Lipid Deposition

The lipid deposition in kidney tissue and HK-2 cells was determined using triglyceride (TG) quantitative assays and Oil Red O staining as previously described [9,23].

2.6 Immunohistochemical and Immunofluorescence Staining

Immunohistochemical staining of kidney tissue and immunofluorescence staining of HK-2 cells were performed by applying previously described methods [23]. Primary antibodies of transforming growth factor-beta 1 (TGF-β1, 1:400, bs-0086R, Bioss, Beijing, China), connective tissue growth factor (CTGF, bs-0743R, 1:400; Bioss), mitofusin 2 (Mfn2, 1:200, 9482S, Cell Signaling Technology, Danvers, MA, USA), and dynamin-related protein 1 (Drp1, 1:200, ab184247, Abcam, Cambridge, UK) were used for immunohistochemical staining. Primary antibody of HIF-1α (1:200, ab179483, Abcam) was used for immunofluorescence staining.

Table 1. Primer sequences used for RT-qPCR.

Gene	Primers sequences (5′-3′)
Drp1	TCACCCGGAGACCTCTCATTC-sense
	GGTTCAGGGCTTACTCCCTTAT-antisense
Mfn2	CTCTCGATGCAACTCTATCGTC-sense
	TCCTGTACGTGTCTTCAAGGA-antisense
OPA1	TGTGAGGTCTGCCAGTCTTTA-sense
	TGTCCTTAATTGGGGTCGTTG-antisense
GAPDH	CTGCACCACCAACTGCTTAG-sense
	AGGTCCACCACTGACACGTT-antisense

2.7 Real-Time Quantitative Polymerase Chain Reaction (RT-qPCR) and Western Blot

Total cellular RNA was extracted from HK-2 cells utilizing TRIzol reagent (9109, TaKaRa, Shiga, Japan) for subsequent RT-qPCR analysis. Then reverse transcripted to cDNA with a commercially available kit (R323-01, Vazyme, Nanjing, Jiangsu, China). Next, Quantitative amplification of target transcripts was subsequently performed

Table 2. Primer sequences used for mitochondrial DNA (mtDNA) quantification.

Gene	Species	Primers sequences (5′-3′)
ND2	Homo sapiens	ACTGCGCTAAGCTCGCACTGATTT-sense
		GATTATGGATGCGGTTGCTTGCGT-antisense
ND2	*Rattus norvegicus*	AGTTGGGAGGAAAGCGGTAG-sense
		CCCTCACCATATTCCCAACCA-antisense
β-actin	Homo sapiens	AAAGACCTGTACGCCAACAC-sense
		GTCATACTCCTGCTTGCTGAT-antisense
β-actin	*Rattus norvegicus*	TTTCCAGCCTTCCTTGGGTATG-sense
		CACTGTGTTGGCATAGAGGTCTTTAC-antisense

on a Bio-Rad thermocycler with gene-specific primers and SYBR green PCR Master Mix (Q711-02, Vazyme). Relative mRNA expression was determined through the comparative $2^{-\Delta\Delta CT}$ approach. Primer sequences utilized for human gene detection are listed in Table 1.

We conducted Western blot experiments following protocols outlined in our earlier publication [22]. Incubation with primary antibodies targeted HIF-1α (1:1000, ab179483, Abcam), Drp1 (1:1000, ab184247, Abcam), Mfn2 (1:1000, 9482S, Cell Signaling Technology), TGF-β1 (1:1000, bs-0086R, Bioss), CTGF (1:1000, bs-0743R, Bioss), and β-actin (1:1000, AF5003, Beyotime).

2.8 Cell Counting Kit-8 (CCK-8) Assay

Cell survival rates were evaluated through CCK-8 colorimetric assay (BS350B, Biosharp, Hefei, Anhui, China) following standard procedures. In brief, cells were seeded at roughly 2000 cells per well in 96-well plates and allowed to grow for 24 h prior to analysis. After synchronized, the cells were treated with emodin (0, 5, 10, 20, 40, 60, 80, and 100 µM) dissolved in DMSO for 6 h. Then, the supernatant containing emodin or DMSO was discarded, followed by adding 10 µL of CCK-8 reagent into each well for 2 h. Finally, optical density readings were then acquired using a multi-mode microplate reader (Thermo Fisher Scientific, Waltham, MA, USA).

2.9 Assessment of Mitochondrial Homeostasis

The adenosine triphosphate (ATP) content in kidney tissues was evaluated using a commercial kit (E-BC-K157-M, Elabscience).

Total DNA isolation from renal tissues and HK-2 cells was accomplished utilizing a commercial extraction kit (DP304, Tiangen, Beijing, China). Then, the gene NADH dehydrogenase subunit-2 (*ND2*) of mitochondrial DNA (mtDNA) was amplified using the real-time quantitative PCR method previously described. The sequences of rat and human primers are shown in Table 2.

Mitochondrial transmembrane potential was evaluated through 5,5′,6,6′-Tetrachloro-1,1′,3,3′-tetraethylbenzimidazolylcarbocyanine iodide (JC-1) staining methodology (E-CK-A301, Elabscience). Briefly, adherent cells from six-well plates were detached, pelleted, and suspended in loading buffer before exposure to JC-1 dye for 20 minutes at 37 °C. After dual washing steps, samples were re-suspended in chilled 1× assay buffer. Acquisition of fluorescent signals was performed on a BD Accuri C6 flow cytometer (BD, Franklin Lakes, NJ, USA). Red emission (575 nm, FL2) indicated JC-1 aggregate formation in viable cells with intact mitochondrial polarization, whereas green emission (525 nm, FL1) signified monomeric JC-1 accumulation in cells with compromised membrane potential.

2.10 Statistical Analysis

Statistical analyses were conducted with GraphPad Prism 8.0 (GraphPad Software, San Diego, CA, USA) or SPSS 22.0 (IBM Corporation, Armonk, NY, USA). Data are presented as mean ± SD. Comparisons between two groups were performed using two-tailed unpaired *t*-test, while one-way ANOVA coupled with Tukey's post-hoc test was employed for multi-group analyses. Statistical significance was set at $p < 0.05$.

3. Results

3.1 Emodin Alleviated Tubular Damage in Diabetic Kidneys

Emodin treatment significantly decreased the ratio of kidney weight to body weight, the 24-h urinary total protein levels, and the ratio of urinary albumin to creatinine in rats with diabetes (Fig. 1A–C), but did not affect blood urea nitrogen levels (Fig. 1D). Meanwhile, the body weights, and serum glucose levels in diabetic rats were not significantly changed by emodin treatment (Fig. 1E,F), suggesting that emodin did not improve kidney damage by affecting blood glucose level. PAS staining showed that emodin treatment rescued the pathological injury of renal tubules in diabetic rats (Fig. 1G,H), characterized by reduced glycogen deposition, attenuated luminal dilation, and less extensive epithelial cell detachment and necrosis. Consistently, the protein expression levels of TGF-β1 and CTGF in the kidneys of rats in the DM + emodin group significantly decreased compared with those in the DM group, suggesting that the degree of renal fibrosis in rats with diabetes was alleviated by emodin administration (Fig. 1I,J).

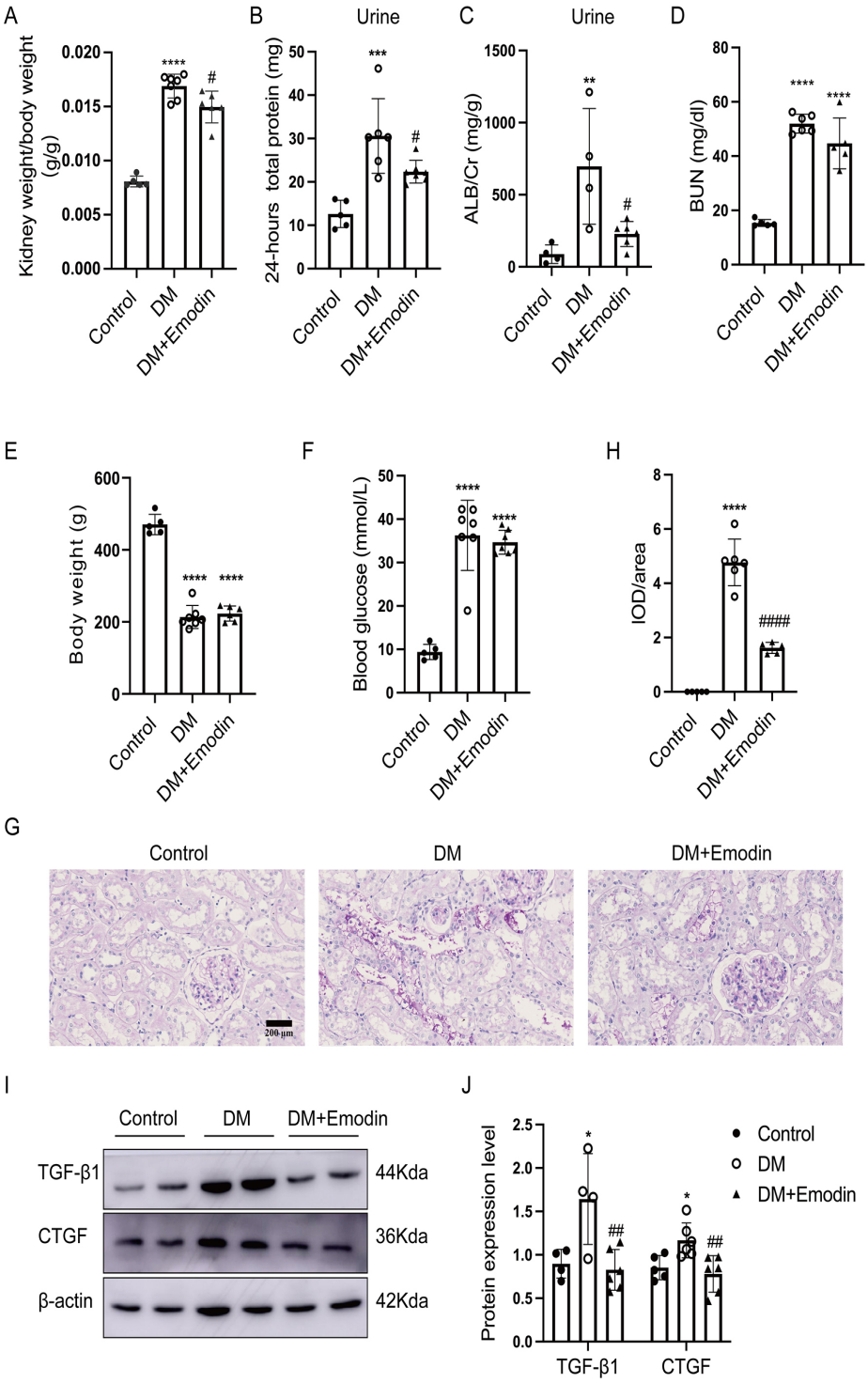

Fig. 1. Emodin alleviated tubular damage in diabetic kidneys. (A) Ratio of kidney weight to body weight (n = 5–7), (B) 24-h total protein levels in urine (n = 5–7), (C) urinary albumin-to-creatinine ratio (n = 4–6), (D) blood urea nitrogen levels (n = 5–6), (E) body weights (n = 5–7), (F) blood glucose levels (n = 5–7) were measured. (G,H) PAS staining (original magnification 400×, scale bar 200 μm). The tubular damage area was quantified using the software Image-Pro Plus (n = 5–6), IOD/area represents the integrated optical density per unit area, serving as an indicator of mean PAS-positive staining intensity. (I,J) For protein expression analysis, Western blot was employed to assess TGF-β1 and CTGF levels in renal tissue, with β-actin serving as an internal normalization standard. Densitometric analysis of protein bands was carried out using ImageJ (n = 4–6). Data are expressed as mean ± SD. Statistical significance relative to the Control group is indicated as $^{*}p < 0.05$, $^{**}p < 0.01$, $^{***}p < 0.001$, $^{****}p < 0.0001$; comparisons against the DM group are denoted by $^{\#}p < 0.05$, $^{\#\#}p < 0.01$, $^{\#\#\#\#}p < 0.0001$. DM, Diabetic Model; PAS, Periodic Acid-Schiff; IOD, Integrated Optical Density; TGF-β1, Transforming Growth Factor-beta 1; CTGF, Connective Tissue Growth Factor.

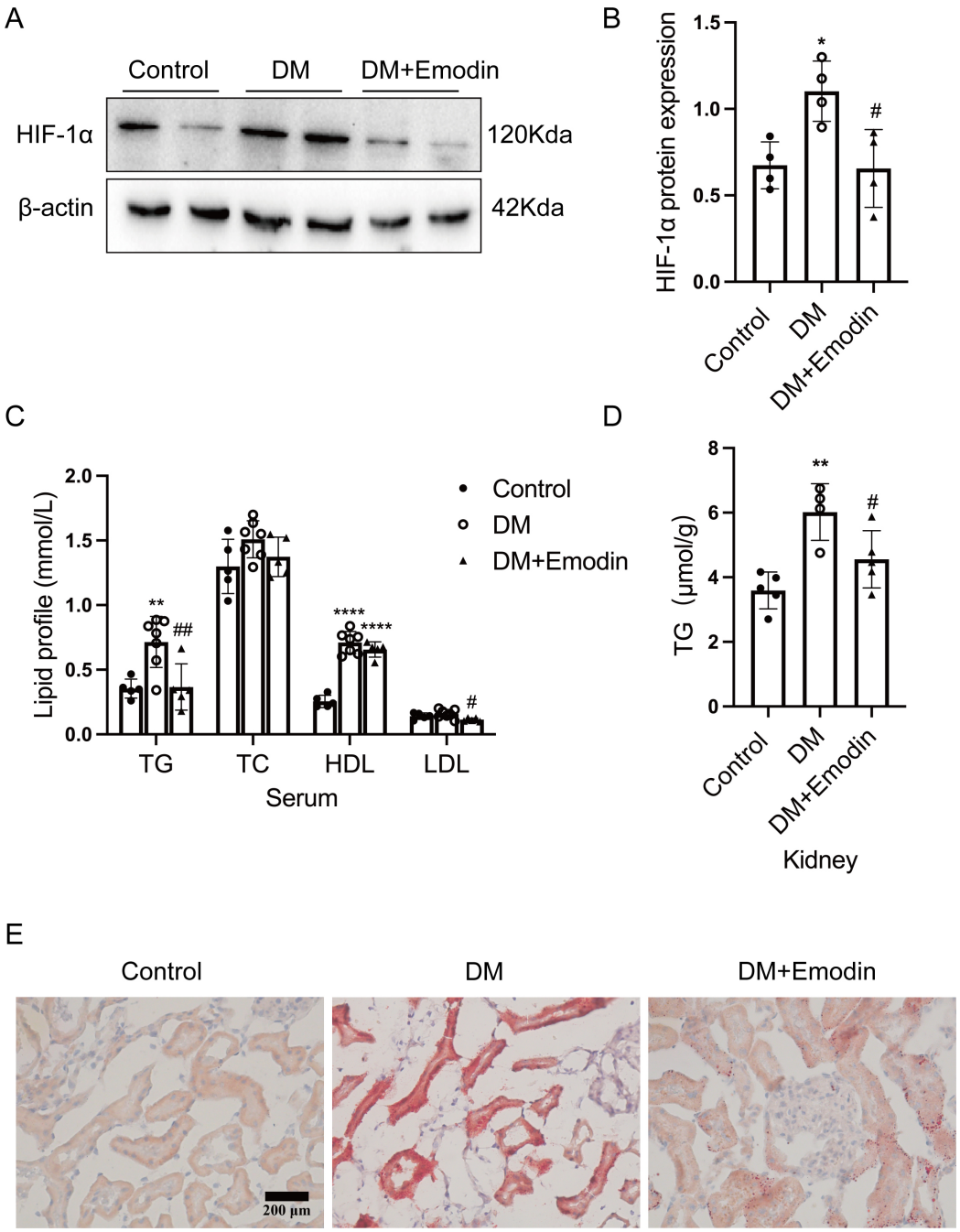

Fig. 2. Emodin decreased lipid deposition in the kidneys of rats with diabetes by inhibiting HIF-1α expression. (A,B) Western blot was conducted to evaluate HIF-1α abundance in renal tissue, with β-actin serving as an internal normalization standard. Densitometric analysis of protein bands was carried out using ImageJ ($n = 4$). (C) Serum lipid profiles were measured ($n = 5$–7). (D) TG quantification assay was performed to detect the TG content in the kidneys ($n = 4$–5). (E) Neutral lipid deposition in kidney sections was visualized by Oil Red O staining (400× magnification; scale bar = 200 µm). Data are expressed as mean ± SD. Statistical significance relative to the Control group is indicated as $^{*}p < 0.05$, $^{**}p < 0.01$, $^{****}p < 0.0001$; comparisons against the DM group are denoted by $^{\#}p < 0.05$, $^{\#\#}p < 0.01$. DM, Diabetic Model; HIF-1α, Hypoxia-Inducible Factor-1 alpha; HDL, High-density lipoprotein; LDL, low-density lipoprotein; TC, total cholesterol; TG, triglyceride.

3.2 Emodin Decreased Lipid Accumulation in Diabetic Kidneys by Suppressing HIF-1α Expression

Hou and colleagues showed that emodin inhibited HIF-1α expression at the translational level [11]. As demonstrated by Western blot, emodin treatment markedly decreased HIF-1α protein expression in the kidneys of rats with diabetes (Fig. 2A,B). The serum lipid profile results showed that emodin administration significantly reduced

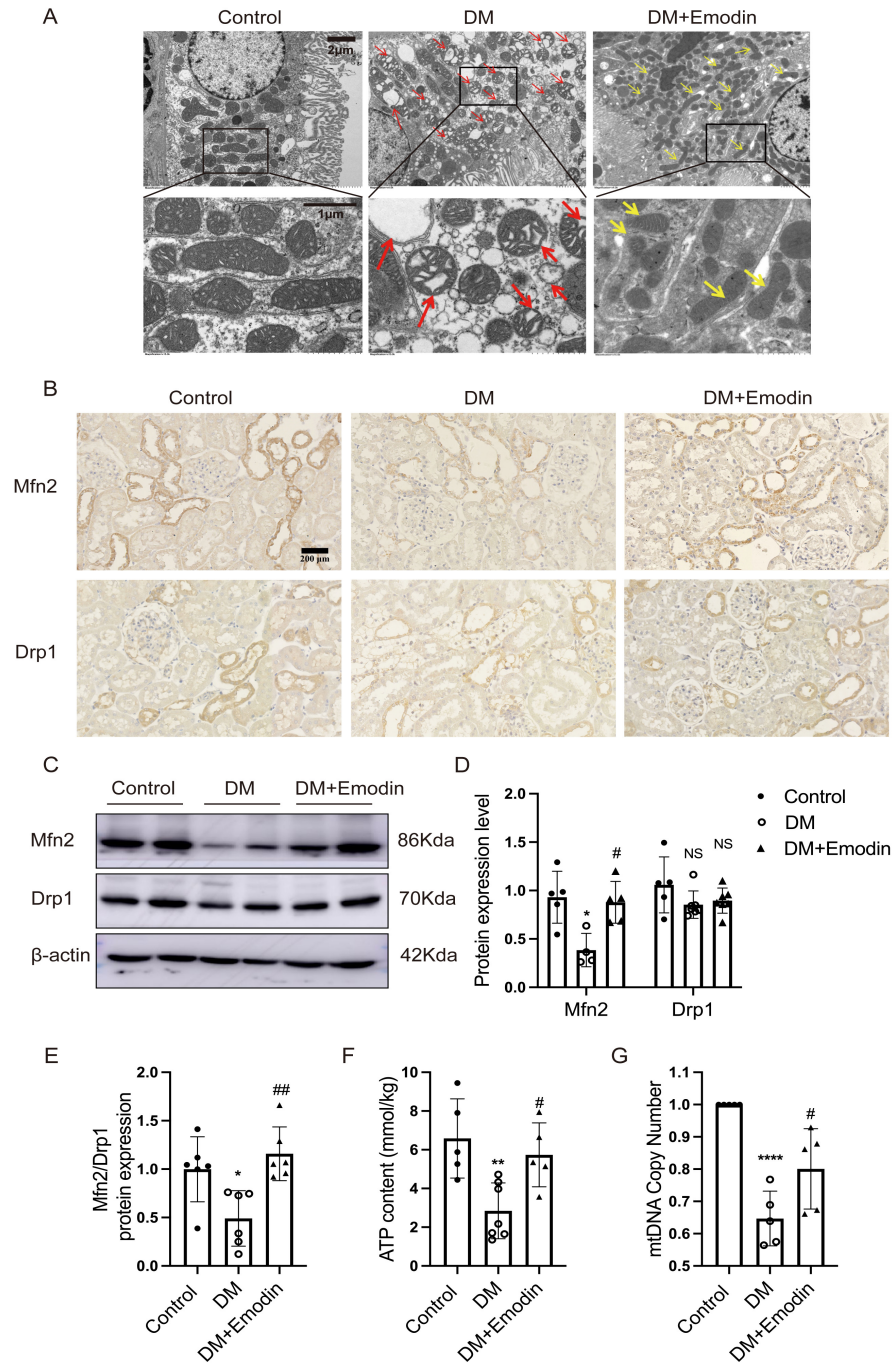

Fig. 3. Emodin improved mitochondrial damage in the tubules of diabetic kidneys. (A) Representative transmission electron microscopy image of tubular epithelial cells in rats. The red arrows indicate damaged mitochondria and their cristae, whereas the yellow arrows indicate improved mitochondria and their cristae (4000× magnification, scale bar = 2 μm; 15,000× magnification scale bar = 1 μm). (B) Protein expression of Mfn2 and Drp1 in the kidneys was shown using immunohistochemistry staining (400× magnification, scale bar = 200 μm). (C,D) Western blot was conducted to evaluate the protein expression of Mfn2 and Drp1 in renal tissue, with β-actin serving as an internal normalization standard. Densitometric analysis of protein bands was carried out using ImageJ (n = 4–7). (E) Ratio of Mfn2 and Drp1 protein expression levels in kidneys was calculated to indicate the degree of mitochondrial fragmentation (n = 6). (F) ATP content of the kidneys was measured (n = 5–7). (G) mtDNA copy numbers of the kidneys were measured by real-time quantitative PCR of ND2 (n = 5). Data are expressed as mean ± SD. Statistical significance relative to the Control group is indicated as $^{*}p < 0.05$, $^{**}p < 0.01$, $^{****}p < 0.0001$, NS (No Significance); comparisons against the DM group are denoted by $^{\#}p < 0.05$, $^{\#\#}p < 0.01$, NS (No Significance). DM, Diabetic Model; Mfn2, Mitofusin 2; Drp1, Dynamin-Related Protein 1; ATP, Adenosine Triphosphate; mtDNA, Mitochondrial DNA; *ND2*, NADH Dehydrogenase 2.

low-density lipoprotein (LDL) and TG levels, but had no effect on the total cholesterol (TC) and high-density lipoprotein (HDL) levels in rats with diabetes (Fig. 2C). The results of TG quantitative assay and Oil Red O staining showed that emodin treatment decreased lipid accumulation in the kidneys of rats with diabetes (Fig. 2D,E). These results suggested that emodin reduced lipid deposition in diabetic kidneys, possibly by inhibiting HIF-1α protein expression.

3.3 Emodin Improved Mitochondrial Damage in the Tubules of Diabetic Kidneys

It was revealed that the mitochondrial damage mediated by HIF-1α activation aggravated cellular injury [24]. It showed that most mitochondria in RTECs of rats with diabetes appeared fragmented, with fractured cristae and vesiculated matrix. Some mitochondria even appeared vacuolated, with swelling and rupture, losing their structural integrity (Fig. 3A). Emodin treatment improved the morphology and structure of mitochondria in RTECs of rats with diabetes (Fig. 3A). Additionally, we quantified the expression of mitochondrial dynamics regulators, specifically Mfn2 and Drp1. Immunohistochemical staining indicated that treatment with emodin normalized the suppressed expression of the fusion-associated protein Mfn2 in diabetic rat kidneys, though no comparable effect was observed on the fission-related protein Drp1 across experimental cohorts (Fig. 3B). The Western blot results were consistent with immunohistochemical staining findings (Fig. 3C,D). However, the ratio of Mfn2 to Drp1 expression levels markedly reduced in the kidneys of rats in the DM group compared with the control group, which was restored after emodin treatment (Fig. 3E). Besides, decreased ATP content and mtDNA copy number in rats with diabetes were rescued by emodin treatment (Fig. 3F,G), indicating that emodin restored energy production and mitochondrial biogenesis in rats with diabetes.

3.4 Emodin Attenuated Lipid Deposition and Cellular Damage in $CoCl_2$_Treated HK-2 Cells by Inhibiting HIF-1α Expression

Based on CCK-8 assay results, emodin at a concentration of 20 µM was selected as the optimal intervention concentration for HK-2 cells (Fig. 4A). Western blot and immunofluorescence staining revealed that $CoCl_2$ stimulation markedly increased HIF-1α expression in the nucleus of HK-2 cells, which was significantly downregulated by emodin treatment (Fig. 4B–D). Meanwhile, emodin intervention substantially attenuated $CoCl_2$-triggered lipid deposition in HK-2 cells (Fig. 4E,F). Furthermore, the upregulated expression of profibrotic mediators TGF-β1 and CTGF in $CoCl_2$-exposed HK-2 cells was significantly suppressed following emodin application. (Fig. 4G,H). These results revealed that emodin effectively ameliorated lipid accumulation and cellular injury in $CoCl_2$-treated HK-2 cells, possibly by inhibiting HIF-1α expression.

3.5 Emodin Ameliorated Mitochondrial Dysfunction in $CoCl_2$-Treated HK-2 Cells

The mRNA expression levels of *Drp1*, *Mfn2*, and *OPA1* significantly decreased in $CoCl_2$-treated HK-2 cells, which were rescued by emodin treatment (Fig. 5A–C). The protein expression of the mitochondrial fusion protein Mfn2 was reduced in $CoCl_2$-treated HK-2 cells but was markedly restored by emodin treatment. While no significant difference was observed in the expression levels of mitochondrial fission protein Drp1 among the three groups (Fig. 5D,E). However, the ratio of Mfn2 to Drp1 expression levels still significantly diminished in $CoCl_2$-treated HK-2 cells compared with those in the control group, which was restored after emodin treatment (Fig. 5F). These results suggested that emodin improved mitochondrial dynamics disorder by regulating the ratio of Mfn2 to Drp1 protein expression levels. Moreover, this treatment reversed the reduction of mtDNA copy number (Fig. 5G) and the loss of mitochondrial membrane potential (Fig. 5H,I) in $CoCl_2$-treated HK-2 cells.

4. Discussion

Although traditional Chinese medicine plays a vital role in DN therapies, its underlying mechanisms in treating DN need exploration to promote its clinical application [25,26]. Emodin has been reported to prevent DN progression through ameliorating podocyte and mesangial cell injury [17,27–30]. Emodin treatment suppressed podocyte apoptosis and boosted autophagy of podocytes in diabetic kidneys [17,27]. Besides, *in vivo* and *in vitro* studies indicated that fibrotic protein expression and cell proliferation in mesangial cells were inhibited by emodin [28–30]. The present study was novel in demonstrating that emodin protected against DN in rat models by mitigating lipid accumulation and cellular injury of tubular epithelial cells. The results showed that the pathological damage of tubules in rats with diabetes was obviously alleviated, accompanied by significantly decreased lipid accumulation after emodin treatment.

Emodin exerted beneficial effects on lipid metabolism in multiple disease models, including obesity, atherosclerosis, severe acute pancreatitis, and nonalcoholic fatty liver disease [14,15,31,32]. Yu *et al.* [15] demonstrated that emodin reduced lipid deposition in the adipose tissue of mice by promoting M2 macrophage polarization. Also, emodin protected hepatocytes against lipid deposition in nonalcoholic fatty liver disease via downregulating cholesterol absorption, decreasing lipid synthesis [32,33]. However, the lipid-modulating effect of emodin in DN requires elucidation. This study showed that emodin treatment significantly downregulated serum TG and LDL levels in rats with DN and inhibited lipid accumulation in diabetic kidneys, which was consistent with the lipid-lowering effect of emodin on other disease models. Besides, these results suggested that emodin did not improve serum lipid profiles

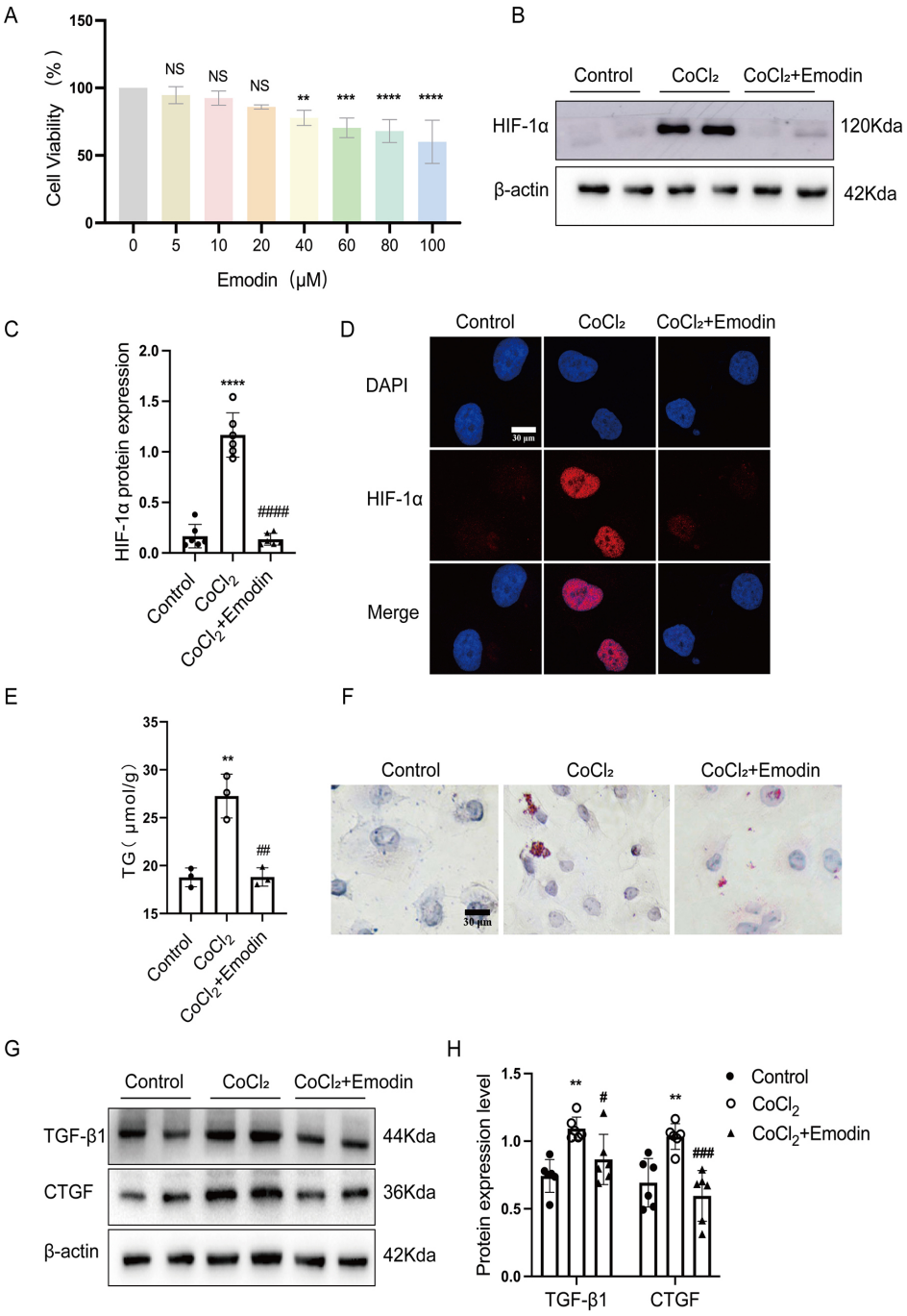

Fig. 4. Emodin attenuated lipid deposition and cellular damage in $CoCl_2$–treated HK-2 cells by inhibiting HIF-1α expression. (A) Cell viability of emodin-treated HK-2 cells with gradually increasing concentrations detected using the CCK-8 kit. (B,C) Western blot was conducted to evaluate HIF-1α abundance in HK-2 cells. (D) Immunofluorescence staining was used to reveal the cellular localization and protein expression level of HIF-1α (scale bar = 30 μm, original magnification 800×). (E) TG quantification assay was performed to detect the TG content in HK-2 cells. (F) Oil Red O staining was used to observe neutral lipid accumulation in HK-2 cells (scale bar = 30 μm, original magnification 200×). (G,H) Western blot analysis was conducted to evaluate the protein expression of TGF-β1 and CTGF in HK-2 cells. β-actin was used as a loading control. Densitometric analysis of protein bands was carried out using ImageJ. All experiments were performed with n $\geq$ 3 biological replicates, $\geq$2 technical replicates per biological replicate, and independently repeated three times. Results are presented as mean $\pm$ SD. Statistical significance relative to the Control group is indicated as $^{**}p < 0.01$, $^{***}p < 0.001$, $^{****}p < 0.0001$, NS (No Significance); comparisons against the $CoCl_2$ group are denoted by $^{\#}p < 0.05$, $^{\#\#}p < 0.01$, $^{\#\#\#}p < 0.001$, $^{\#\#\#\#}p < 0.0001$. $CoCl_2$, Cobalt Chloride; CCK-8, Cell Counting Kit-8; HIF-1α, Hypoxia-Inducible Factor-1 alpha; TGF-β1, Transforming Growth Factor-beta 1; CTGF, Connective Tissue Growth Factor; TG, Triglyceride.

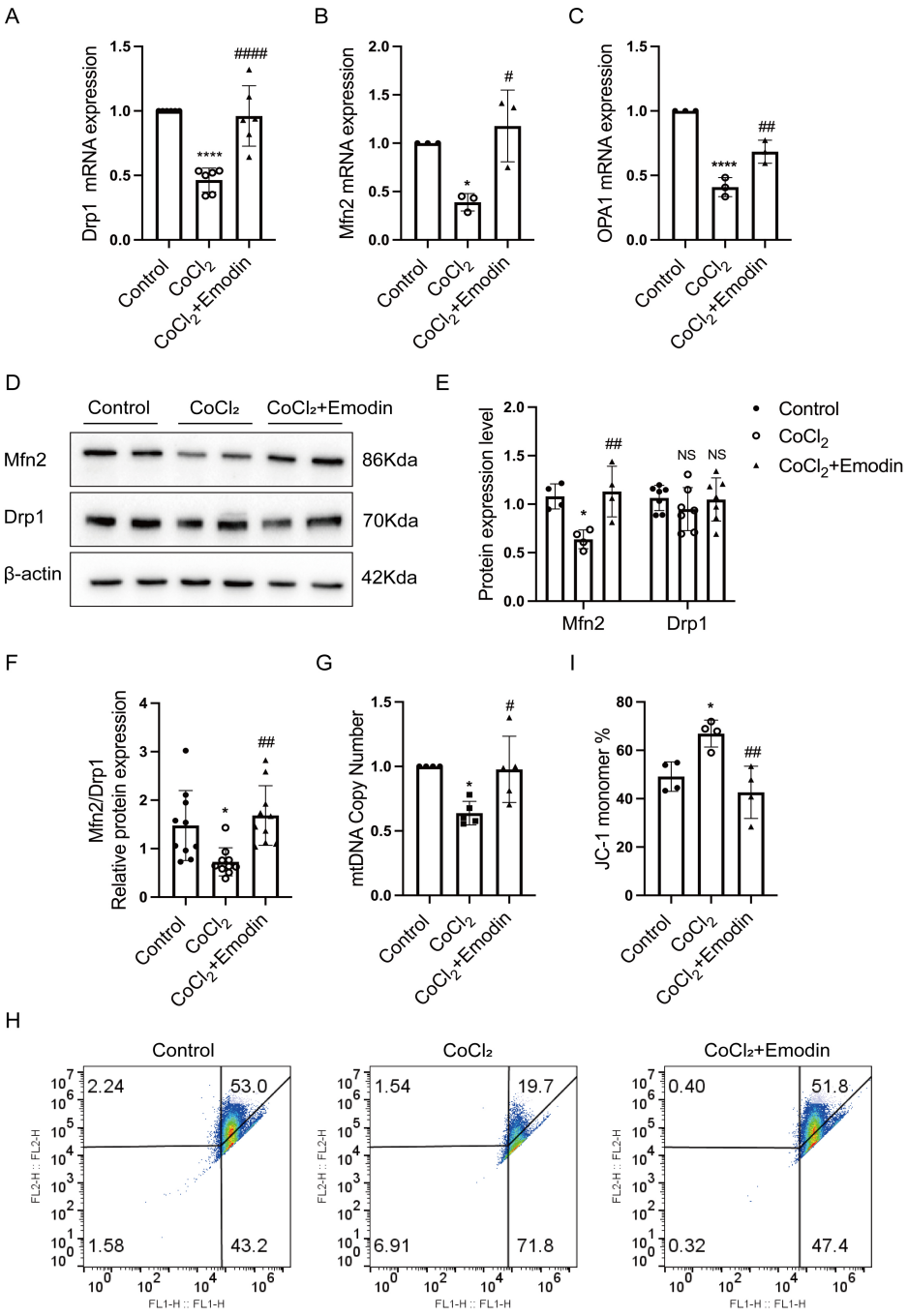

Fig. 5. Emodin ameliorated mitochondrial dysfunction in $CoCl_2$–treated HK-2 cells. (A–C) Real-time quantification PCR was performed to detect the mRNA expression of *Drp1*, *Mfn2*, and *OPA1* in HK-2 cells. (D,E) Western blot was conducted to evaluate of Mfn2 and Drp1 protein expression in HK-2 cells, with β-actin serving as an internal normalization standard. Densitometric analysis of protein bands was carried out using ImageJ (F) The Mfn2-to-Drp1 expression ratio was computed to assess the extent of mitochondrial fragmentation in HK-2 cells. (G) For mtDNA quantification, real-time PCR targeting ND2 was performed in HK-2 cells. (H,I) Mitochondrial membrane potential of HK-2 cells was evaluated by flow cytometric analysis, with subsequent data processing conducted using FlowJo. All experiments were performed with n $\geq$ 3 biological replicates, $\geq$2 technical replicates per biological replicate, and independently repeated three times. Data are expressed as mean $\pm$ SD. Statistical significance relative to the Control group is indicated as $^{*}p < 0.05$, $^{****}p < 0.0001$, NS (No Significance); comparisons against the $CoCl_2$ group are denoted by $^{\#}p < 0.05$, $^{\#\#}p < 0.01$, $^{\#\#\#\#}p < 0.0001$, NS (No Significance). $CoCl_2$, Cobalt Chloride; Drp1, Dynamin-Related Protein 1; Mfn2, Mitofusin 2; OPA1, Optic Atrophy 1; mtDNA, Mitochondrial DNA; *ND2*, NADH Dehydrogenase 2; JC-1, 5,5′,6,6′-Tetrachloro-1,1′,3,3′-tetraethylbenzimidazolylcarbocyanine iodide.

in rats with DN by promoting ectopic lipid deposition in kidneys, but simultaneously improved them both.

It is noteworthy that despite significant kidney protective effects, emodin treatment did not achieve glycemic control in our study. This dissociation between renal and metabolic outcomes suggests that emodin's beneficial effects on kidney function may operate through HIF-1α-mediated mechanisms that are independent of systemic glucose homeostasis. However, we cannot exclude the possibility that more prolonged metabolic dysregulation might eventually compromise renal function, or that glycemic control could become relevant in longer-term studies. Future investigations should explore whether combination therapy with glucose-lowering agents could produce synergistic renal benefits.

Emodin protects RTECs from pathological damage via multiple mechanisms. Liu and colleagues revealed that emodin hindered epithelial–mesenchymal transdifferentiation by enhancing autophagy through upregulating the expression of bone morphogenic protein 7 in renal fibrosis [34]. Wang *et al*. [35] identified the miR-490-3p/HMGA2 signaling axis as the mechanistic conduit through which emodin exerts renoprotective effects, specifically attenuating tubular epithelial cell damage in fibrotic kidney disease. Moreover, the *in vitro* study showed that emodin prevented cellular damage from hypoxia/reoxygenation by downregulating oxidative stress and apoptosis in HK-2 cells [36]. Consistent with the aforementioned findings, our study confirmed that emodin effectively reduced RTECs injury *in vivo* and *in vitro*. Moreover, our results revealed that emodin prevented lipid accumulation and cellular injury by inhibiting HIF-1α expression in the tubules of rats with DN, highlighting the mechanism of action of emodin in DN therapy. However, this study did not comprehensively investigate whether emodin protects RTECs through modulating other signaling pathways involved in DN pathogenesis (e.g., including oxidative stress, inflammation, and Ang-II). This constitutes a significant limitation of the present study.

Previous studies suggested that mitochondrial homeostasis imbalance exacerbated cellular lipid deposition [37–39]. The present study showed that emodin treatment mitigated structural and functional imbalance of mitochondria *in vivo* and *in vitro*, suggesting that emodin might alleviate lipid accumulation and cellular injury in diabetic tubules through reversing mitochondrial homeostasis. HIF-1α activation promoted mitochondrial homeostasis dysfunction in various disease states [24,40–42]. Also, owing to the inhibitory effect of emodin on HIF-1α expression observed in this study, we proposed that emodin might reverse mitochondrial homeostasis, thereby protecting against diabetic tubular injury via inhibiting HIF-1α expression.

5. Limitations

We acknowledge two important limitations of this study. First, the present study employed standard oral administration as a proof-of-concept to demonstrate pharmacological efficacy in diabetic nephropathy; However, translation to clinical practice will require formulation optimization because emodin has poor oral bioavailability and low aqueous solubility. Recent advances demonstrate that nano-drug delivery systems (liposomes, polymeric nanoparticles, nanogels) can significantly enhance emodin solubility and bioavailability [43], while structural modifications and material-based targeted delivery strategies offer additional avenues to overcome pharmacokinetic limitations [44]. Second, this study used established urinary biomarkers to assess renal injury. While clinically validated, these markers may be affected by reporting quality issues, and our targeted approach excludes the comprehensive profiling achievable through "omics" technologies. Future multi-omics integration could enhance diagnostic and mechanistic insights.

6. Conclusions

In summary, this study was novel in demonstrating that emodin prevented lipid accumulation and cellular injury in RTECs of diabetic kidneys. Emodin inhibited excessive HIF-1α activation, thus exerting a protective effect on mitochondria.

Availability of Data and Materials

All data used and analyzed during this study will be available from the corresponding author upon reasonable request.

Author Contributions

YW and XD performed the research, conducted the data analysis, and wrote the manuscript. QZ and JZ assisted in conducting the animal experiments. ZQ, FG and SZ assisted in cell culture. CW, LW, SL participated in research design and data interpretation. ZH designed the work and conducted manuscript polishing. All authors contributed to editorial changes in the manuscript. All authors read and approved the final manuscript. All authors have participated sufficiently in the work and agreed to be accountable for all aspects of the work.

Ethics Approval and Consent to Participate

The animal protocols used in current study were approved by the Laboratory Animal Welfare and Ethics Committee of Wannan Medical University (No. LLSC-2022-212), and the experimental procedures were conducted in accordance with the *Guide for the Care and Use of Laboratory Animals*.

Acknowledgment

Not applicable.

Funding

This study was supported by the Excellent Youth Research Project in Anhui Province's Universities (Grant No. 2024AH030056), the National Natural Science Foundation of China Youth Fund (Grant No. 82000698), the Wuhu City Basic Research on the Application of Science and Technology Projects under Grant 2022jc28, the Wannan Medical University Doctoral Research Initiation Fund (Grant No. WYRCQD2019007), and the Anhui Province College Students' Innovation and Entrepreneurship Training Program Project (Grant No. S202410368007).

Conflict of Interest

The authors declare no conflict of interest.

References

[1] Sagoo MK, Gnudi L. Diabetic Nephropathy: An Overview. Methods in Molecular Biology (Clifton, N.J.). 2020; 2067: 3–7. https://doi.org/10.1007/978-1-4939-9841-8_1.

[2] Zhang Y, Jin D, Kang X, Zhou R, Sun Y, Lian F, *et al*. Signaling Pathways Involved in Diabetic Renal Fibrosis. Frontiers in Cell and Developmental Biology. 2021; 9: 696542. https://doi.org/10.3389/fcell.2021.696542.

[3] Schelling JR. The Contribution of Lipotoxicity to Diabetic Kidney Disease. Cells. 2022; 11: 3236. https://doi.org/10.3390/cells11203236.

[4] Kimmelstiel P, Wilson C. Intercapillary Lesions in the Glomeruli of the Kidney. The American Journal of Pathology. 1936; 12: 83–98.7.

[5] Wang XX, Jiang T, Shen Y, Caldas Y, Miyazaki-Anzai S, Santamaria H, *et al*. Diabetic nephropathy is accelerated by farnesoid X receptor deficiency and inhibited by farnesoid X receptor activation in a type 1 diabetes model. Diabetes. 2010; 59: 2916–2927. https://doi.org/10.2337/db10-0019.

[6] Wang Z, Jiang T, Li J, Proctor G, McManaman JL, Lucia S, *et al*. Regulation of renal lipid metabolism, lipid accumulation, and glomerulosclerosis in FVBdb/db mice with type 2 diabetes. Diabetes. 2005; 54: 2328–2335. https://doi.org/10.2337/diabetes.54.8.2328.

[7] Khan S, Abu Jawdeh BG, Goel M, Schilling WP, Parker MD, Puchowicz MA, *et al*. Lipotoxic disruption of NHE1 interaction with PI(4,5)P2 expedites proximal tubule apoptosis. The Journal of Clinical Investigation. 2014; 124: 1057–1068. https://doi.org/10.1172/JCI71863.

[8] Lee LE, Doke T, Mukhi D, Susztak K. The key role of altered tubule cell lipid metabolism in kidney disease development. Kidney International. 2024; 106: 24–34. https://doi.org/10.1016/j.kint.2024.02.025.

[9] Hu Z, Zhu Q, Wang Y, Deng X, Yang H, Zhou M, *et al*. Lipid nephrotoxicity mediated by HIF-1α activation accelerates tubular injury in diabetic nephropathy. Renal Failure. 2024; 46: 2347446. https://doi.org/10.1080/0886022X.2024.2347446.

[10] Li L, Tian Y, Yu J, Song X, Jia R, Cui Q, *et al*. iTRAQ-based quantitative proteomic analysis reveals multiple effects of Emodin to Haemophilus parasuis. Journal of Proteomics. 2017; 166: 39–47. https://doi.org/10.1016/j.jprot.2017.06.020.

[11] Hou H, Li D, Cheng D, Li L, Liu Y, Zhou Y. Cellular Redox Status Regulates Emodin-Induced Radiosensitization of Nasopharyngeal Carcinoma Cells In Vitro and In Vivo. Journal of Pharmaceutics. 2013; 2013: 218297. https://doi.org/10.1155/2013/218297.

[12] Ma F, Hu L, Yu M, Wang F. Emodin Decreases Hepatic Hypoxia-Inducible Factor-1[Formula: see text] by Inhibiting its Biosynthesis. The American Journal of Chinese Medicine. 2016; 44: 997–1008. https://doi.org/10.1142/S0192415X16500555.

[13] Cheng L, Zhang S, Shang F, Ning Y, Huang Z, He R, *et al*. Emodin Improves Glucose and Lipid Metabolism Disorders in Obese Mice *via* Activating Brown Adipose Tissue and Inducing Browning of White Adipose Tissue. Frontiers in Endocrinology. 2021; 12: 618037. https://doi.org/10.3389/fendo.2021.618037.

[14] Song H, Zhang J, Lou N, Jiang X, Cui Y, Liu J, *et al*. Emodin nanocapsules inhibit acute pancreatitis by regulating lipid metabolic reprogramming in macrophage polarization. Phytomedicine: International Journal of Phytotherapy and Phytopharmacology. 2024; 130: 155763. https://doi.org/10.1016/j.phymed.2024.155763.

[15] Yu F, Yu N, Peng J, Zhao Y, Zhang L, Wang X, *et al*. Emodin inhibits lipid accumulation and inflammation in adipose tissue of high-fat diet-fed mice by inducing M2 polarization of adipose tissue macrophages. FASEB Journal: Official Publication of the Federation of American Societies for Experimental Biology. 2021; 35: e21730. https://doi.org/10.1096/fj.202100157RR.

[16] Zeng JY, Wang Y, Miao M, Bao XR. The Effects of Rhubarb for the Treatment of Diabetic Nephropathy in Animals: A Systematic Review and Meta-analysis. Frontiers in Pharmacology. 2021; 12: 602816. https://doi.org/10.3389/fphar.2021.602816.

[17] Liu H, Wang Q, Shi G, Yang W, Zhang Y, Chen W, *et al*. Emodin Ameliorates Renal Damage and Podocyte Injury in a Rat Model of Diabetic Nephropathy via Regulating AMPK/mTOR-Mediated Autophagy Signaling Pathway. Diabetes, Metabolic Syndrome and Obesity: Targets and Therapy. 2021; 14: 1253–1266. https://doi.org/10.2147/DMSO.S299375.

[18] Ji J, Tao P, Wang Q, Cui M, Cao M, Xu Y. Emodin attenuates diabetic kidney disease by inhibiting ferroptosis via upregulating Nrf2 expression. Aging. 2023; 15: 7673–7688. https://doi.org/10.18632/aging.204933.

[19] Li J, Ding L, Song B, Xiao X, Qi M, Yang Q, *et al*. Emodin improves lipid and glucose metabolism in high fat diet-induced obese mice through regulating SREBP pathway. European Journal of Pharmacology. 2016; 770: 99–109. https://doi.org/10.1016/j.ejphar.2015.11.045.

[20] Dong X, Wen R, Xiong Y, Jia X, Zhang X, Li X, *et al*. Emodin alleviates CRS4-induced mitochondrial damage via activation of the PGC1α signaling. Phytotherapy Research: PTR. 2024; 38: 1345–1357. https://doi.org/10.1002/ptr.8091.

[21] Jing D, Bai H, Yin S. Renoprotective effects of emodin against diabetic nephropathy in rat models are mediated via PI3K/Akt/GSK-3β and Bax/caspase-3 signaling pathways. Experimental and Therapeutic Medicine. 2017; 14: 5163–5169. https://doi.org/10.3892/etm.2017.5131.

[22] Hu ZB, Ma KL, Zhang Y, Wang GH, Liu L, Lu J, *et al*. Inflammation-activated CXCL16 pathway contributes to tubulointerstitial injury in mouse diabetic nephropathy. Acta Pharmacologica Sinica. 2018; 39: 1022–1033. https://doi.org/10.1038/aps.2017.177.

[23] Hu ZB, Lu J, Chen PP, Lu CC, Zhang JX, Li XQ, *et al*. Dysbiosis of intestinal microbiota mediates tubulointerstitial injury in diabetic nephropathy via the disruption of cholesterol homeostasis. Theranostics. 2020; 10: 2803–2816. https://doi.org/10.7150/thno.40571.

[24] Wang YW, Dong HZ, Tan YX, Bao X, Su YM, Li X, *et al*. HIF-1α-regulated lncRNA-TUG1 promotes mitochondrial dysfunction and pyroptosis by directly binding to FUS in myocardial infarction. Cell Death Discovery. 2022; 8: 178. https://doi.org/10.1038/s41420-022-00969-8.

[25] Shen S, Zhong H, Zhou X, Li G, Zhang C, Zhu Y, *et al*. Advances in Traditional Chinese Medicine research in diabetic kidney disease treatment. Pharmaceutical Biology. 2024; 62: 222–232. https://doi.org/10.1080/13880209.2024.2314705.

[26] Zhang J, Cao P, Gui J, Wang X, Han J, Wang Y, *et al*. Arctigenin ameliorates renal impairment and inhibits endoplasmic reticulum stress in diabetic db/db mice. Life Sciences. 2019; 223: 194–201. https://doi.org/10.1016/j.lfs.2019.03.037.

[27] Chen T, Zheng LY, Xiao W, Gui D, Wang X, Wang N. Emodin ameliorates high glucose induced-podocyte epithelial-mesenchymal transition in-vitro and in-vivo. Cellular Physiology and Biochemistry: International Journal of Experimental Cellular Physiology, Biochemistry, and Pharmacology. 2015; 35: 1425–1436. https://doi.org/10.1159/000373963.

[28] Gao J, Wang F, Wang W, Su Z, Guo C, Cao S. Emodin suppresses hyperglycemia-induced proliferation and fibronectin expression in mesangial cells via inhibiting cFLIP. PloS One. 2014; 9: e93588. https://doi.org/10.1371/journal.pone.0093588.

[29] Yang J, Zeng Z, Wu T, Yang Z, Liu B, Lan T. Emodin attenuates high glucose-induced TGF-β1 and fibronectin expression in mesangial cells through inhibition of NF-κB pathway. Experimental Cell Research. 2013; 319: 3182–3189. https://doi.org/10.1016/j.yexcr.2013.10.006.

[30] Li X, Liu W, Wang Q, Liu P, Deng Y, Lan T, *et al*. Emodin suppresses cell proliferation and fibronectin expression via p38MAPK pathway in rat mesangial cells cultured under high glucose. Molecular and Cellular Endocrinology. 2009; 307: 157–162. https://doi.org/10.1016/j.mce.2009.03.006.

[31] Luo N, Fang J, Wei L, Sahebkar A, Little PJ, Xu S, *et al*. Emodin in atherosclerosis prevention: Pharmacological actions and therapeutic potential. European Journal of Pharmacology. 2021; 890: 173617. https://doi.org/10.1016/j.ejphar.2020.173617.

[32] Hu N, Liu J, Xue X, Li Y. The effect of emodin on liver disease – comprehensive advances in molecular mechanisms. European Journal of Pharmacology. 2020; 882: 173269. https://doi.org/10.1016/j.ejphar.2020.173269.

[33] Meng J, Xu J, Yang S, Liu W, Zeng J, Shi L, *et al*. Emodin lows NPC1L1-mediated cholesterol absorption as an uncompetitive inhibitor. Bioorganic & Medicinal Chemistry Letters. 2022; 75: 128974. https://doi.org/10.1016/j.bmcl.2022.128974.

[34] Liu W, Gu R, Lou Y, He C, Zhang Q, Li D. Emodin-induced autophagic cell death hinders epithelial-mesenchymal transition via regulation of BMP-7/TGF-β1 in renal fibrosis. Journal of Pharmacological Sciences. 2021; 146: 216–225. https://doi.org/10.1016/j.jphs.2021.03.009.

[35] Wang L, Wang X, Li G, Zhou S, Wang R, Long Q, *et al*. Emodin ameliorates renal injury and fibrosis *via* regulating the miR-490-3p/HMGA2 axis. Frontiers in Pharmacology. 2023; 14: 1042093. https://doi.org/10.3389/fphar.2023.1042093.

[36] Chen H, Huang RS, Yu XX, Ye Q, Pan LL, Shao GJ, *et al*. Emodin protects against oxidative stress and apoptosis in HK-2 renal tubular epithelial cells after hypoxia/reoxygenation. Experimental and Therapeutic Medicine. 2017; 14: 447–452. https://doi.org/10.3892/etm.2017.4473.

[37] Zhou Y, Liu L, Jin B, Wu Y, Xu L, Chang X, *et al*. Metrnl Alleviates Lipid Accumulation by Modulating Mitochondrial Homeostasis in Diabetic Nephropathy. Diabetes. 2023; 72: 611–626. https://doi.org/10.2337/db22-0680.

[38] Sun Y, Ge X, Li X, He J, Wei X, Du J, *et al*. High-fat diet promotes renal injury by inducing oxidative stress and mitochondrial dysfunction. Cell Death & Disease. 2020; 11: 914. https://doi.org/10.1038/s41419-020-03122-4.

[39] Su Y, Tang M, Wang M. Mitochondrial Dysfunction of Astrocytes Mediates Lipid Accumulation in Temporal Lobe Epilepsy. Aging and Disease. 2024; 15: 1289–1295. https://doi.org/10.14336/AD.2023.0624.

[40] Xiao Y, Liu X, Xie K, Luo J, Zhang Y, Huang X, *et al*. Mitochondrial dysfunction induced by HIF-1α under hypoxia contributes to the development of gastric mucosal lesions. Clinical and Translational Medicine. 2024; 14: e1653. https://doi.org/10.1002/ctm2.1653.

[41] Liu H, Wu X, Yang T, Wang C, Huang F, Xu Y, *et al*. NARFL deficiency caused mitochondrial dysfunction in lung cancer cells by HIF-1α-DNMT1 axis. Scientific Reports. 2023; 13: 17176. https://doi.org/10.1038/s41598-023-44418-7.

[42] Teng H, Wu D, Lu L, Gao C, Wang H, Zhao Y, *et al*. Design and synthesis of 3,4-seco-lupane triterpene derivatives to resist myocardial ischemia-reperfusion injury by inhibiting oxidative stress-mediated mitochondrial dysfunction via the PI3K/AKT/HIF-1α axis. Biomedicine & Pharmacotherapy. 2023; 167: 115452. https://doi.org/10.1016/j.biopha.2023.115452.

[43] Ai Z, Liu B, Chen J, Zeng X, Wang K, Tao C, *et al*. Advances in nano drug delivery systems for enhanced efficacy of emodin in cancer therapy. International Journal of Pharmaceutics: X. 2024; 9: 100314. https://doi.org/10.1016/j.ijpx.2024.100314.

[44] Zheng Q, Li S, Li X, Liu R. Advances in the study of emodin: an update on pharmacological properties and mechanistic basis. Chinese Medicine. 2021; 16: 102. https://doi.org/10.1186/s13020-021-00509-z.